Journal of Computational Physics 228 (2009) 2604–2615

Contents lists available at ScienceDirect

Journal of Computational Physics

journal homepage: www.elsevier.com/locate/jcp

Explicit time-reversible orbit integration in Particle In Cell codes with static homogeneous magnetic field

L. Patacchini *, I.H. Hutchinson

Plasma Science and Fusion Center, Department of Nuclear Science and Engineering, Massachusetts Institute of Technology (MIT), NW21 Albany Street, Cambridge, 02139 MA, USA

ARTICLE INFO

Article history:
Received 6 November 2007
Received in revised form 31 October 2008
Accepted 18 December 2008
Available online 27 December 2008

Keywords:
Boris
Symplectic
Integrator
Particle In Cell
Plasma
Magnetic field

ABSTRACT

A new explicit time-reversible orbit integrator for the equations of motion in a static homogeneous magnetic field – called Cyclotronic integrator – is presented. Like Spreiter and Walter's Taylor expansion algorithm, for sufficiently weak electric field gradients this second order method does not require a fine resolution of the Larmor motion; it has however the essential advantage of being symplectic, hence time-reversible. The Cyclotronic integrator is only subject to a linear stability constraint ($\Omega\Delta t < \pi$, Ω being the Larmor angular frequency), and is therefore particularly suitable to electrostatic Particle In Cell codes with uniform magnetic field where Ω is larger than any other characteristic frequency, yet a resolution of the particles' gyromotion is required. Application examples and a detailed comparison with the well-known (time-reversible) Boris algorithm are presented; it is in particular shown that implementation of the Cyclotronic integrator in the kinetic codes SCEPTIC and Democritus can reduce the cost of orbit integration by up to a factor of ten.

1. Introduction

The Boris integration scheme [1], designed to solve the single particle equations of motion in electric and magnetic fields

$$\begin{cases} \dot{\mathbf{x}} = \mathbf{v} \\ m\dot{\mathbf{v}} = Q(\mathbf{E} + \mathbf{v} \wedge \mathbf{B}) \end{cases} \tag{1}$$

is perhaps the most widely used orbit integrator in explicit Particle In Cell (PIC) simulations of plasmas; here $\mathbf{x}$ and $\mathbf{v}$ are the particle position and velocity, m its mass and Q its charge. The idea of the Boris integrator is to offset $\mathbf{x}$ and $\mathbf{v}$ by half a time-step $\Delta t/2$, and update them alternately using the following *Drift* (D) and *Kick* (K) operators:

$$D_B(\Delta t) := \mathbf{x}' - \mathbf{x} = \Delta t \mathbf{v}, \tag{2}$$

$$K_B(\Delta t) := \mathbf{v}' - \mathbf{v} = \Delta t \frac{Q}{m}\left[\mathbf{E}(\mathbf{x}') + \frac{\mathbf{v}' + \mathbf{v}}{2} \wedge \mathbf{B}(\mathbf{x}')\right]. \tag{3}$$

Although seemingly implicit (the right hand side of Eq. (3) contains both $\mathbf{v}$ and $\mathbf{v}'$, the velocities at the beginning and end of the step), K_B can easily be inverted and the scheme is in practice explicit. The reasons for Boris scheme's popularity are twofold.

* Corresponding author.
E-mail address: patacchi@mit.edu (L. Patacchini).

0021-9991/$ - see front matter © 2009 Elsevier Inc. All rights reserved.
doi:10.1016/j.jcp.2008.12.021

It must first be recognized that the algorithm is extremely simple to implement, and offers second order accuracy while requiring only one force (or field) evaluation per time-step. Other integrators such as the usual or midpoint second order Runge–Kutta [2] require two such evaluations per step, thus considerably increasing the computational cost. The second reason is that for stationary electric and magnetic fields, the errors on conserved quantities such as the energy, or the canonical angular momentum when the system is axisymmetric, are bounded for an infinite time (the error on those quantities is second order in Δt as is the scheme). Those conservation properties, usually observed on long-time simulations of periodic or quasi-periodic orbits, are characteristic of time-reversible integrators [3].

Unfortunately the Boris scheme requires a fine resolution of the Larmor angular frequency $\Omega = Q|\mathbf{B}|/m$, typically $\Omega\Delta t \lesssim 0.3$ for a 1% accuracy [1], which is penalizing if Ω is much larger than any other characteristic frequency of the problem. In the regime of static uniform magnetic field considered in this paper, Spreiter and Walter [4] previously attempted to relax the Larmor constraint, and developed a "Taylor expansion algorithm". Their method however suffers from non time-reversibility, as well as a "weak" unconditional unstability particularly apparent when $\Omega\Delta t \lesssim O(1)$.

We developed an alternative integrator by taking advantage of the fact that in a uniform magnetic field and zero electric field the particle trajectory has a simple analytic form. Using this method, called Cyclotronic integrator, the time-step is in theory only limited by linear stability considerations (leading to $\Omega\Delta t < \pi$). By construction, in static uniform magnetic fields the Cyclotronic integrator is second order and symplectic [5]; in other words it preserves the geometric structure of the Hamiltonian flow, which guarantees excellent conservation properties. The authors' main motivation for the present work was to increase the speed of electrostatic PIC codes such as SCEPTIC [6,7] or Democritus [8], designed to study the electrostatic flow of a uniform magnetoplasma past an electrode. For this system, it is indeed necessary to resolve the Larmor rotation in order to accurately compute the orbit intersections with the collector. The appropriate time-step regime is $\Omega\Delta t \lesssim O(1)$; Spreiter and Walter's algorithm can therefore not be used because of its unstability, while the Boris scheme is too expensive for strongly magnetized plasmas. The Cyclotronic integrator can also be useful to the simulation of other systems, such as intermediately magnetized Penning traps where the magnetic field is not strong enough for a guiding-center approach to be applicable [9].

The paper is organized as follows: After a review of Boris and Spreiter and Walter's algorithms (Section 2), we present a construction of the Cyclotronic integrator where its symplectic character straightforwardly appears (Section 3). A linear stability analysis of the these algorithms is performed in Section 4. We then proceed with the application of the Cyclotronic integrator to the ideal Penning trap system (Section 5) and to the PIC codes SCEPTIC and Democritus (Section 6).

2. Review of previous integrators

2.1. Boris integrator

The Boris integrator [1] is a time-splitting method; the equations of motion (1) are separated in two parts that are successively integrated in a Verlet form:

$$\begin{pmatrix}\mathbf{x}\\ \mathbf{v}\end{pmatrix}(t+\Delta t) = D_B(\Delta t/2)\cdot K_B(\Delta t)\cdot D_B(\Delta t/2)\begin{pmatrix}\mathbf{x}\\ \mathbf{v}\end{pmatrix}(t), \tag{4}$$

where the Boris Drift and Kick operators (D_B and K_B) are defined in Eqs. (2) and (3). If $\overline{\overline{R}}_{\Delta\boldsymbol{\varphi}}$ denotes a rotation of characteristic vector

$$\Delta\boldsymbol{\varphi} = 2\mathrm{atan}\left(\frac{\Delta t}{2}\Omega\right)\frac{\mathbf{B}}{B}, \tag{5}$$

$K_B(\Delta t)$: $= \mathbf{v} \to \mathbf{v}'$ can be split in the following way [1]:

$$K_B(\Delta t) := \begin{cases}\mathbf{v}^* = \mathbf{v} + \frac{Q\mathbf{E}\Delta t}{2m},\\ \mathbf{v}^{**} = \overline{\overline{R}}_{\Delta\boldsymbol{\varphi}}\mathbf{v}^*,\\ \mathbf{v}' = \mathbf{v}^{**} + \frac{Q\mathbf{E}\Delta t}{2m}.\end{cases} \tag{6}$$

Eqs. (2) and (6) readily show that the Boris integrator is time-reversible, even for non uniform magnetic fields. Indeed the Drift operator does not act on the particle velocity, and the Kick operator does not act on the position. In PIC codes it is customary to define the position and velocity with half a time-step of offset, which amounts to concatenating the two adjacent $D_B(\Delta t/2)$ from successive steps in Eq. (4).

A popular variant of this integrator (known as the "tan" transformation [1]), second order in Δt, consists in letting $\Delta\boldsymbol{\varphi} = \Omega\Delta t\frac{\mathbf{B}}{B}$ in Eq. (6). Regardless of the form used for $\Delta\boldsymbol{\varphi}$ however, the Drift operator (2) requires $\Omega\Delta t \ll \pi$, which is a severe limitation if the other characteristic frequencies (such as the quadrupole harmonic frequency ω_0 introduced in Section 4, or the plasma frequency in dynamic systems) are much smaller than Ω.

2.2. Spreiter and Walter's Taylor expansion algorithm

An intuitive way to build an orbit integrator for Eq. (1) with homogeneous magnetic field, not subject to the Larmor constraint, is to take advantage of the available analytic form of a charged particle's trajectory in uniform electric and magnetic fields. In the plane normal to $\mathbf{B} = B\mathbf{e}_z$, using the complex notation for the perpendicular part of the vectors ($\underline{x} = x + iy, \underline{v} = v_x + iv_y$ and $\underline{E} = E_x + iE_y$) [4]:

$$\underline{v}(t+\Delta t) = \left(\underline{v}(t) + i\frac{\underline{E}}{B}\right)\exp(-i\Omega\Delta t) - i\frac{\underline{E}}{B}, \tag{7}$$

$$\underline{x}(t+\Delta t) = \underline{x}(t) + \frac{i}{\Omega}\left(\underline{v}(t) + i\frac{\underline{E}}{B}\right)[\exp(-i\Omega\Delta t) - 1] - i\frac{\underline{E}}{B}\Delta t. \tag{8}$$

If the electric field is non uniform, the scheme provided by Eqs. (7) and (8) is second order accurate for the position and first order accurate for the velocity. In the same regime of homogeneous magnetic field, Spreiter and Walter derived a one-step integrator (Eqs. (28)–(35) in Ref. [4]) based on a Taylor expansion of the equations of motion (1) in which $\Omega\Delta t$ is not assumed to be small. Their integrator is equivalent to Eqs. (7) and (8), with a corrective term added to Eq. (8) in order for the velocity update to be second order accurate.

In a uniform electric field, Spreiter and Walter's algorithm integrates the exact orbit regardless of the time-step. Because the electric field at the beginning and end of each time-step does not enter the propagation equations symmetrically, it is unfortunately not time-reversible.

3. Derivation of the Cyclotronic integrator

3.1. Symplectic and time-reversible integration

Time-reversible integrators contain the subclass of symplectic schemes, which has received considerable attention in the last decades in particular in connection with astrodynamics [10] and accelerator physics [11].

The fundamental idea behind symplectic integration of (systems of) Ordinary Differential Equations (ODEs) is to ensure that the chosen scheme is a canonical map, in other words that there exist canonical coordinates $(\mathbf{q},\mathbf{p})$ related to the physical variables $(\mathbf{x},\mathbf{v})$ such that the flow $Z(\tau) = (\mathbf{q},\mathbf{p})(\tau)$ derives from a Hamiltonian $\widetilde{H}$:

$$\frac{d\mathbf{p}}{dt} = -\nabla_{\mathbf{q}}\widetilde{H} \quad \frac{d\mathbf{q}}{dt} = \nabla_{\mathbf{p}}\widetilde{H}, \tag{9}$$

in which case there exists a Liouville operator $\Psi_{\widetilde{H}}$ such that

$$\frac{dZ}{dt} = \{Z, \widetilde{H}(Z)\} = \Psi_{\widetilde{H}}Z \tag{10}$$

or equivalently

$$\forall\tau \in \mathbf{R} \quad z(\tau) = e^{\tau\Psi_{\widetilde{H}}}Z(0), \tag{11}$$

where $\{\cdot,\cdot\}$ stands for the Poisson bracket. Indeed if the original ODEs derive from a Hamiltonian $H(\mathbf{q},\mathbf{p})$, one can show that the Hamiltonian from which the flow of a consistent nth order symplectic integrator derives takes the form: $\widetilde{H}(\mathbf{q},\mathbf{p}) = H(\mathbf{q},\mathbf{p}) + \delta H(\mathbf{q},\mathbf{p},\Delta t)$, where $\delta\mathrm{H} = O(\Delta t^n)$ [12]. Because the integrator exactly preserves $\widetilde{H}$ and its integral invariants, it is expected to conserve slightly modified expressions of the integral invariants of H. Hence no secular drift in the original problem's energy or integral invariants is to occur. For a more complete introduction on symplectic integration avoiding unnecessary mathematical formalism, the reader is referred to Ref. [5].

The Boris integrator is known for its outstanding conservation properties. However, as pointed out by Stoltz et al. [13], there is no guarantee that it is symplectic. It is nonetheless time-reversible, and it has been shown under very reasonable assumptions that this condition is sufficient to explain the absence of secular drift in the conserved quantities, provided the orbit we integrate is periodic or quasi-periodic [3].

3.2. Cyclotronic integrator

The time independent Hamiltonian for single particle motion in the presence of a uniform background magnetic field $\mathbf{B} = B\mathbf{e}_z$ can easily be written in cylindrical coordinates:

$$H(\mathbf{q},\mathbf{p}) = \frac{p_\rho^2}{2m} + \frac{p_z^2}{2m} + \frac{1}{2m}\left(\frac{p_\varphi}{\rho} - QA_\varphi(\rho,z)\right)^2 + Q\phi(\mathbf{q}), \tag{12}$$

where the generalized momentum $\mathbf{p}$ is given by

$$\begin{cases} p_z = m\dot{z}, \\ p_\rho = m\dot{\rho}, \\ p_\varphi = m\rho^2\left(\dot{\varphi} + Q\frac{A_\varphi}{m\rho}\right), \end{cases} \tag{13}$$

and $\mathbf{q} = (z, \rho, \varphi)$. The vector potential $\mathbf{A}$ satisfies $\nabla \wedge \mathbf{A} = B\mathbf{e_z}$ and is chosen to be $\mathbf{A} = \frac{B\rho}{2}\mathbf{e}_\varphi$, while $\mathbf{E} = -\nabla\phi$.

The flow deriving from the full Hamiltonian H in Eq. (12) is not integrable. It is however possible to rewrite H as $H = H_1 + H_2$ where the flows associated with $H_{1,2}$ are exactly integrable for any time-step Δt as follows:

- Drift part: $H_1(\mathbf{q},\mathbf{p}) = \frac{p_\rho^2}{2m} + \frac{p_z^2}{2m} + \frac{1}{2m}\left(\frac{p_\varphi}{\rho} - QA_\varphi(\rho,z)\right)^2$. Uniform helical motion around $\mathbf{B}$ with angle $\Delta\boldsymbol{\varphi} = \Omega\Delta t\frac{\mathbf{B}}{B}$.
- Kick part: $H_2(\mathbf{q},\mathbf{p}) = Q\phi(\mathbf{q})$. Momentum increase of vector $-Q\nabla\boldsymbol{\phi}\Delta t$.

Using the Baker Campbell Hausdorff formula [5], one can show that

$$e^{\Delta t\Psi_H} = e^{(\Delta t/2)\Psi_{H1}} \cdot e^{\Delta t\Psi_{H2}} \cdot e^{(\Delta t/2)\Psi_{H1}} + \mathrm{O}(\Delta t^3). \tag{14}$$

A second order symplectic integrator for H is therefore

$$P_C(\Delta t) = D_C(\Delta t/2) \cdot K_C(\Delta t) \cdot D_C(\Delta t/2), \tag{15}$$

where $D_C(\Delta t)$ and $K_C(\Delta t)$ are the Drift and Kick operators in $(\mathbf{x},\mathbf{v})$ space corresponding to $\exp(\Delta t\Psi_{H1})$ and $\exp(\Delta t\Psi_{H2})$ in $(\mathbf{q},\mathbf{p})$ space.

One can straightforwardly show that (in a homogeneous magnetic field) the Cyclotronic integrator is second order accurate. In addition, in the absence of electric field it is exact regardless of Δt since it exactly resolves the Larmor motion associated with the Hamiltonian H_1. This is of course not the case with the Boris scheme.

A practical implementation in Cartesian coordinates of the Cyclotronic integrator ready to use in PIC codes where $\mathbf{B} = B\mathbf{e}_z$ is given by Eqs. (17) and (18), where the two half Drifts in Eq. (15) have been staggered together. However, because here the Drift operator advances both the position and the velocity, one can not interpret this operation as simply shifting $\mathbf{v}$ and $\mathbf{x}$ by half a time-step. Applying both operators results in $(\mathbf{x},\mathbf{v}) \to (\mathbf{x}',\mathbf{v}') \to (\mathbf{x}'',\mathbf{v}'')$. With $\Delta\boldsymbol{\varphi} = \boldsymbol{\Omega}\Delta t$:

(1) Drift

$$D_C(\Delta t) := \begin{cases} z' = z + v_z\Delta t, \\ (x,y)' = (x,y)_c + R_{\Delta\boldsymbol{\varphi}}((x,y) - (x,y)_c), \\ (v_x, v_y)' = R_{\Delta\boldsymbol{\varphi}}(v_x, v_y), \end{cases} \tag{16}$$

$(x,y)_c(t)$ being the center of the current Larmor circle when any electric field is disregarded. More explicitly:

$$D_C(\Delta t) := \begin{cases} z' - z = v_z\Delta t, \\ x' - x = \frac{v_y - v_y\cos(\Omega\Delta t) + v_x\sin(\Omega\Delta t)}{\Omega}, \\ y' - y = \frac{-v_x + v_x\cos(\Omega\Delta t) + v_y\sin(\Omega\Delta t)}{\Omega}, \\ v_x' = v_x\cos(\Omega\Delta t) + v_y\sin(\Omega\Delta t), \\ v_y' = v_y\cos(\Omega\Delta t) - v_x\sin(\Omega\Delta t). \end{cases} \tag{17}$$

(2) Kick:

$$K_C(\Delta t) := \mathbf{v}'' - \mathbf{v}' = -Q\nabla\phi(\mathbf{x}')\Delta t/m. \tag{18}$$

3.3. Uniform electric field

As a price for their time-reversibility, the Boris and the Cyclotronic integrators don't share Spreiter and Walter's algorithm property of computing the exact orbit in a uniform electric field $\mathbf{E}$. This is not an issue *per se* because a uniform electric field can always be made to vanish by an appropriate change of frame (provided $B \neq 0$ of course). In practice therefore time-steps will be solely limited by electric field gradients.

It is however interesting to notice that although the Cyclotronic integrator does not exactly resolve the motion for non-zero uniform $\mathbf{E}$, it computes an orbit whose Larmor center exactly moves with the drift velocity $\mathbf{E} \wedge \mathbf{B}/B^2$. Fig. 1 shows the orbit calculated with the three integrators assuming $\mathbf{E} = E\mathbf{e}_x$ and a zero initial velocity. For this configuration $\Omega\Delta t$ is the only relevant dimensionless parameter provided velocities are normalized to E/B (the drift velocity); for this example we use $\Omega\Delta t = \pi/2$.

For completeness, we mention that gyrokinetic orbit integrators would also exactly respect the $\mathbf{E} \wedge \mathbf{B}/B^2$ Larmor center motion in the uniform electric field case. However those require $\Omega\Delta t \gg 1$, and are typically used in perturbative particle codes designed to analyze large-scale phenomena such as drift instabilities or zonal flows in Tokamaks [14].

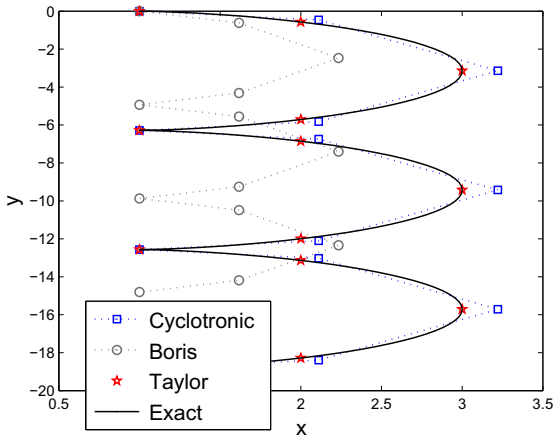

Fig. 1. Orbits computed with the three integrators for $\mathbf{E} = E\mathbf{e}_x$ using a time-step $\Omega\Delta t = \pi/2$, assuming the particle is originally at rest at $(x_0 = 1, y_0 = 0)$. On this illustrative example, no change of frame allowing for the homogeneous electric field to vanish has been operated. It can be seen that the Cyclotronic integrator respects the correct drift velocity $\mathbf{E} \wedge \mathbf{B}/B^2 (= -1 \cdot \mathbf{e}_y$ in dimensionless units). The orbit integrated with the Boris scheme drifts at an incorrect velocity.

4. Linear stability

In addition to being consistent with the original equation, it is desirable that an integration scheme be stable. However, proving that this is the case for arbitrary Ordinary Differential Equations (ODEs) and initial conditions is in general not feasible, and stability properties are therefore usually assessed on linearized forms of the propagation equations. That an orbit integrator be linearly stable for any particle position and time is a necessary condition for its stability in the presence of an arbitrary potential distribution, and is in practice sufficient.

4.1. Linear propagation operators

Let us consider a uniform background magnetic field $\mathbf{B} = B\mathbf{e}_z$, and an ideal quadrupole potential distribution:

$$\phi(\mathbf{r}) = \epsilon \frac{m}{Q}\left(\frac{1}{2}\omega_{0x}^2 x^2 + \frac{1}{2}\omega_{0y}^2 y^2 - \frac{1}{2}(\omega_{0x}^2 + \omega_{0y}^2) z^2\right), \tag{19}$$

where $\epsilon = \pm 1$.

Because transverse and axial dynamics are decoupled, we can concentrate on the transverse motion and treat the problem as two-dimensional; we therefore write the position and velocity evolution between time-steps n and $n+1$ as

$$\begin{pmatrix} x \\ y \\ v_x\Delta t \\ v_y\Delta t \end{pmatrix}^{n+1} = P \begin{pmatrix} x \\ y \\ v_x\Delta t \\ v_y\Delta t \end{pmatrix}^{n}, \tag{20}$$

where P is the linear propagation operator depending on the dimensionless quantities $\epsilon\omega_{0x,y}\Delta t$ and $\Omega\Delta t$. The integration scheme is stable if and only if the spectral radius of P (maximal absolute value of its eigenvalues) satisfies

$$\max(|\mathrm{Sp}(P)|) \leqslant 1. \tag{21}$$

For the Cyclotronic integrator, the operator P_C to be used in Eq. (20) corresponding to Eq. (15) is:

$$P_C(\Delta t) = D_C(\Delta t/2) \cdot K_C(\Delta t) \cdot D_C(\Delta t/2), \tag{22}$$

where (c.f. Eqs. (17) and (18)):

$$D_C(\Delta t/2) = \begin{pmatrix} 1 & 0 & \frac{\sin(\Omega\Delta t/2)}{\Omega\Delta t} & \frac{1-\cos(\Omega\Delta t/2)}{\Omega\Delta t} \\ 0 & 1 & -\frac{1-\cos(\Omega\Delta t/2)}{\Omega\Delta t} & \frac{\sin(\Omega\Delta t/2)}{\Omega\Delta t} \\ 0 & 0 & \cos(\Omega\Delta t/2) & \sin(\Omega\Delta t/2) \\ 0 & 0 & -\sin(\Omega\Delta t/2) & \cos(\Omega\Delta t/2) \end{pmatrix}, \quad K_C(\Delta t) = \begin{pmatrix} 1 & 0 & 0 & 0 \\ 0 & 1 & 0 & 0 \\ -\epsilon\omega_{0x}^2\Delta t^2 & 0 & 1 & 0 \\ 0 & -\epsilon\omega_{0y}^2\Delta t^2 & 0 & 1 \end{pmatrix}. \tag{23}$$

For the Boris integrator, the operator P_B corresponding to Eq. (4) is:

$$P_B(\Delta t) = D_B(\Delta t/2) \cdot K_B(\Delta t) \cdot D_B(\Delta t/2), \tag{24}$$

where $D_B(\Delta t/2)$ is the operator associated with the half Drift:

$$D_B(\Delta t/2) = \begin{pmatrix} 1 & 0 & 1/2 & 0 \\ 0 & 1 & 0 & 1/2 \\ 0 & 0 & 1 & 0 \\ 0 & 0 & 0 & 1 \end{pmatrix}, \tag{25}$$

and $K_B(\Delta t) = K_B{}^a\ (\Delta t/2) \cdot K_B{}^b(\Delta t) \cdot K_B{}^a(\Delta t/2)$ associated with the Kick. $K_B{}^a(\Delta t/2)$ is half the electric part of the Kick and $K_{\text{Boris}}{}^b(\Delta\ t)$ the magnetic part. Using the "tan" modification:

$$K_B^a(\Delta t/2) = \begin{pmatrix} 1 & 0 & 0 & 0 \\ 0 & 1 & 0 & 0 \\ -\epsilon\omega_{0x}^2\Delta t^2/2 & 0 & 1 & 0 \\ 0 & -\epsilon\omega_{0y}^2\Delta t^2/2 & 0 & 1 \end{pmatrix}, \quad K_B^b(\Delta t) = \begin{pmatrix} 1 & 0 & 0 & 0 \\ 0 & 1 & 0 & 0 \\ 0 & 0 & \cos(\Omega\Delta t) & \sin(\Omega\Delta t) \\ 0 & 0 & -\sin(\Omega\Delta t) & \cos(\Omega\Delta t) \end{pmatrix}. \tag{26}$$

Writing the operators in PIC form (one full drift followed by one full Kick) results in different propagation matrices P, but stability conditions are not affected.

4.2. Transversely isotropic harmonic oscillator

If $\epsilon = -1$ the electrostatic force is repulsive in the $\boldsymbol{\rho}$-direction and attractive in the **z**-direction; if in addition $\omega_{0x} = \omega_{0y} = \omega_0$ we simulate an ideal Penning trap system (see Section 5). When $\epsilon = 1$, the opposite holds and the particle is not axially confined (i.e. escapes on the **z**-axis); however in this section we only study the transverse motion and do not worry about **z**-axis stability.

Fig. 2 shows the corresponding linear stability diagrams, and a few important points should be noticed. In the absence of electric field both schemes are stable regardless of $\Omega\Delta t$. In the absence of magnetic field, both schemes are stable if $0 \leqslant \epsilon\omega_0\Delta t \leqslant 2$, which is a well known result [1]. In the limit $|\epsilon\omega_0\Delta t| \ll 1$ with $\epsilon = -1$, the scheme is unstable if $\Omega/\omega_0 < 2$: this is the physical Penning trap instability, and hence independent of the integrator (see Section 5 and Eq. (27)). Reliable orbit integration requires one to operate in the first stability region containing the origin. For $|\omega_0\Delta t|$ small enough, $\Omega\Delta t < 2\pi$ is required.

4.3. Transversely one-dimensional harmonic oscillator

Let us now assume that $\omega_{0y} = 0$. The corresponding stability diagrams are shown in Fig. 3, and are slightly different from the ones in Fig. 2 although the main characteristics are similar. It is interesting to notice that the stability diagram for the Cyclotronic integrator is scaled down by a factor of 2 with respect to the $\omega_{0x} = \omega_{0y}$ case.

For arbitrary physically stable harmonic potentials, numerical stability diagrams are in between the ones shown in Figs. 2 and 3. Because in most of the simulations the potential distribution is not harmonic however, we keep as linear stability

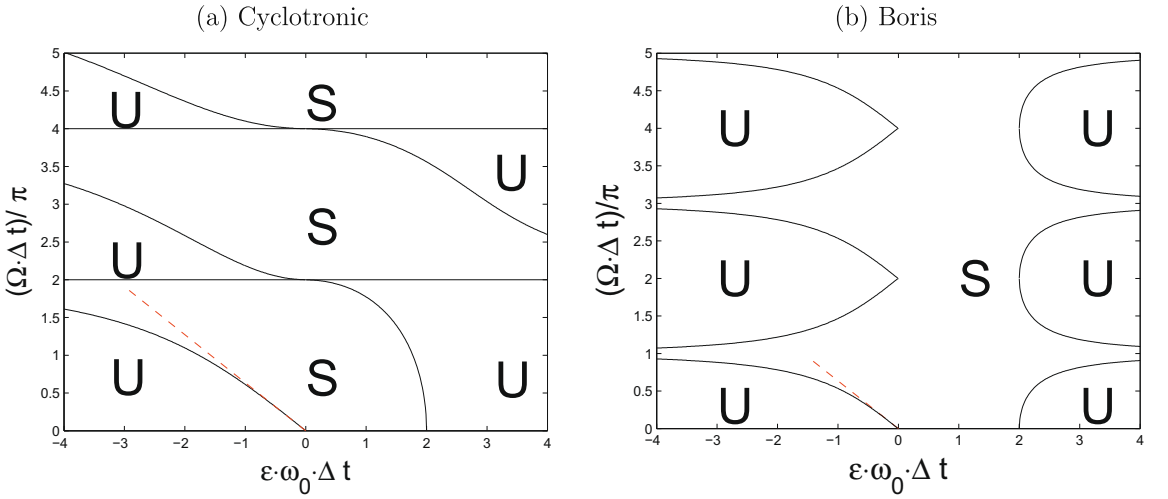

Fig. 2. Linear stability diagrams for the transverse motion (the dynamics along **z** is disregarded) for the Cyclotronic (a) and the Boris (b) integrators, when the harmonic electrostatic force is transversely isotropic (Eq. (19) with $\omega_0 = \omega_{0x} = \omega_{0y}$). "*S*" labels stable regions, and "*U*" unstable regions. The red dashed line is the Penning trap instability (Eq. (27)).

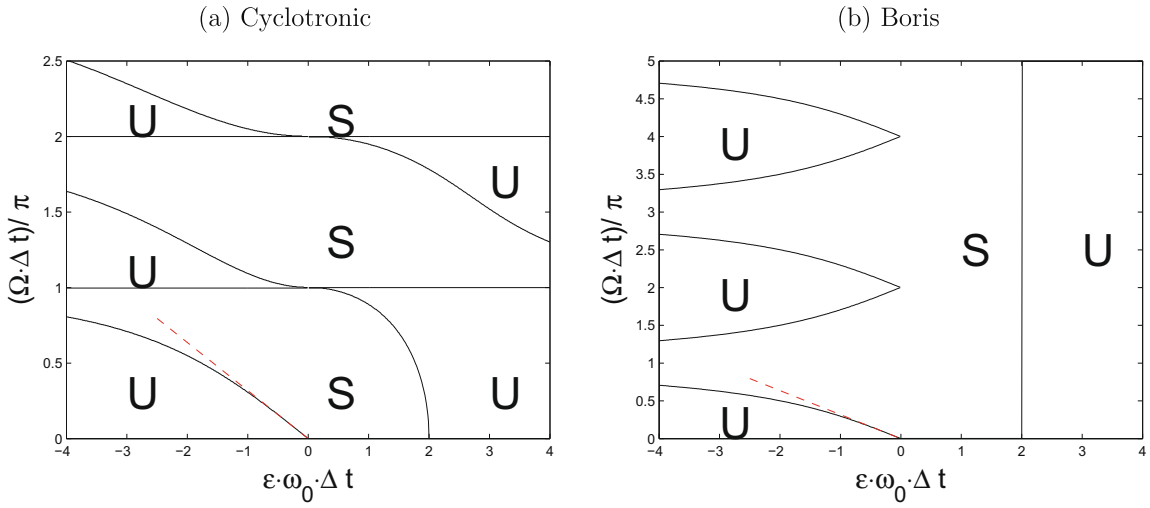

Fig. 3. Idem Fig. 2, but with $\omega_0 = \omega_{0x}$ and $\omega_{0y} = 0$. The red dashed line is a modified Penning trap stability boundary accounting for $\omega_{0y} = 0$, found to be $\Omega/\omega_0 < 1$.

condition the tighter possible linear constraint. In other words for $|\omega_0 \Delta t|$ small enough, in order to avoid islands of instability the time-step should be limited to $\Omega\Delta t < \pi$ (with either Boris or the Cyclotronic schemes).

4.4. Taylor expansion algorithm of Spreiter and Walter

In addition to not being time-reversible, Spreiter and Walter's algorithm has a Jacobian determinant slightly greater than unity [4], which usually leads to instability [2]. It is in fact possible to assert that the scheme is unconditionally unstable for any parameters except if $\Omega\Delta t = 0$ and $0 \leqslant \epsilon\omega_0\Delta t \leqslant 2$, in which case the algorithm is merely the standard unmagnetized leap-frog [1].

As an illustration of this unconditional unstability, Fig. 4 shows contour-lines of $\delta = \max(|\mathrm{Sp}(P_T)|) - 1$, where P_T is the propagation matrix corresponding to the Taylor expansion algorithm in the presence of the electrostatic potential of Eq. (19) with $\omega_{0x} = \omega_{0y} = \omega_0$. P_T is easily obtained from Eqs. (28)–(35) in Ref. [4].

Fig. 4(b) shows that for large $\Omega\Delta t$ the spectral radius contour lines of the Taylor expansion propagator P_T are parabolic (red dotted parabolae: $\Omega\Delta t \propto (\omega_0\Delta t)^2$). In other words for fixed $\omega_0\Delta t$, as $\Omega\Delta t \to \infty$ the scheme tends to stability ($\delta \to 0$). This explains why the authors in Ref. [4] observed that their algorithm performance increases with rising magnetic field.

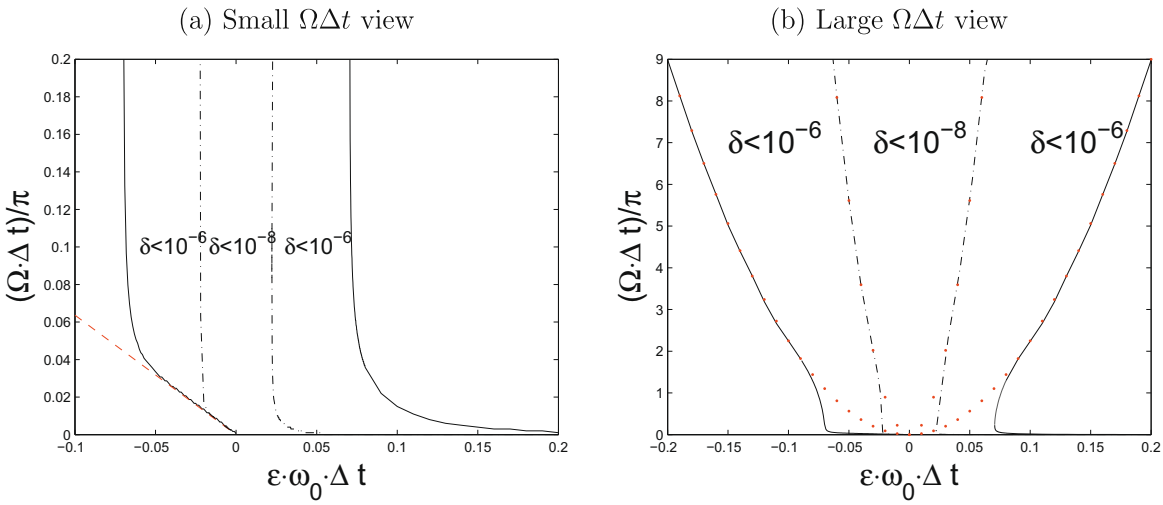

Fig. 4. Contour-plots of $\delta = \max(|\mathrm{Sp}(P_T)|) - 1 = 10^{-6}$ (Solid black line) and $\delta = 10^{-8}$ (Dash-dotted black line) in the vicinity of the origin (a) and for larger $\Omega\Delta t$ (b). The scheme is unconditionally unstable ($\delta > 0$) except for $\Omega\Delta t = 0$ and $0 \leqslant \epsilon\omega_0\Delta t \leqslant 2$ in which case $\delta = 0$. The red dashed line (a) corresponds to the Penning trap instability, and the red dotted parabola (b) to the large $\Omega\Delta t$ limit of the contour-lines.

The Taylor expansion algorithm is therefore a very interesting option when it is appropriate to use $\Omega\Delta t \gg 1$, and provided we do not need to integrate over too long a time-period. For instance if one wishes to integrate 10^6 time-steps, it is approximately necessary to be inside the "$\delta = 10^{-6}$" contour line in Fig. 4(b) whose equation is $\Omega\Delta t \sim 225(\omega_0\Delta t)^2$; in other words $\Omega/\omega_0 \gg 225\omega_0\Delta t$ is required.

A more detailed comparison between this algorithm and the Cyclotronic integrator is presented in Section 5.3.

5. Application 1: the ideal Penning trap

A Penning trap is a cylindrically symmetric device with a static magnetic field along the **z**-axis and a quadrupole electrostatic field of the form of Eq. (19) with $\omega_0 = \omega_{0x} = \omega_{0y}$ and $\epsilon = -1$. Elementary algebra shows that the trap is physically stable if and only if:

$$\Omega \geqslant 2\omega_0, \tag{27}$$

and the orbit is found to be a linear combination of the three following angular frequencies [15]:

$$\begin{cases} \text{Axial} & \omega_0, \\ \text{Modified Cyclotron} & \omega_{\text{MC}} = \frac{\Omega}{2} + \sqrt{\left(\frac{\Omega}{2}\right)^2 - \omega_0^2}, \\ \text{Magnetron} & \omega_{\text{Mag}} = \frac{\Omega}{2} - \sqrt{\left(\frac{\Omega}{2}\right)^2 - \omega_0^2}. \end{cases} \tag{28}$$

In the transverse direction the orbit is a superposition of the fast Modified Cyclotron oscillation and the slow Magnetron motion.

5.1. Frequency shifts

Since the electric field depends linearly on the position, there is no natural scale length and one can consider the position to be dimensionless. Velocities (hence frequencies) are normalized to ω_0.

Fig. 5 shows the particle's numerically-calculated orbit projected on the **x**-axis for two different values of $\Omega\Delta t$, the only physically meaningful quantity Ω/ω_0 being kept fixed ($\Omega/\omega_0 = 10\pi/3$). Fig. 5(a) corresponds to a case where Δt is six times smaller than the Larmor period ($\Omega\Delta t = \pi/3$). The fourth order Runge–Kutta integrator is not satisfactory since it operates as a low-pass filter, and after a few time-steps the Cyclotron oscillation has been damped out: only the Magnetron motion is resolved. The Boris integrator resolves both frequencies but those are offset (The Magnetron frequency shift is clearly visible in the figure.) The Cyclotronic integrator resolves both frequencies as well, but the error is much smaller than with the Boris integrator.

Fig. 5(b) corresponds to $\Omega\Delta t = 3\pi/2$, situation in which the time-step is longer than half the Larmor period. As shown in Section 4.2, both Boris and the Cyclotronic integrators are stable for this choice of time-step; according to the Nyquist theorem however this implies ω_{MC} cannot be properly resolved. Fig. 5(b) should therefore only be considered for illustration purposes, and we never recommend the Cyclotronic integrator with $\Omega\Delta t \geqslant \pi$. Examination of the Magnetron frequencies extracted from the numerical experiment (Table in Fig. 5) shows that while the Cyclotronic integrator introduces less than 2% error, the Boris scheme is in error by a factor of 2.

Fig. 6 shows the fractional error in the characteristic frequencies

$$\text{Fractional Error} = \frac{|\omega_{\text{Output}} - \omega_{\text{Theory}}|}{\omega_{\text{Theory}}} \tag{29}$$

against Δt for $\Omega/\omega_0 = 5\pi/3$. Both integrators appear second order accurate as expected, but the Cyclotronic scheme is one order of magnitude more accurate for ω_{MC} and almost two orders of magnitude more accurate for ω_{Mag}. This accuracy gap increases with the ratio Ω/ω_0, and tends to infinity when $\Omega/\omega_0 \gg 1$. However, if we aim for the typical 1% accuracy on ω_{Mag}, one sees in Fig. 6 that for the Boris scheme $\omega_0\Delta t \sim 0.06$ is required (i.e. $\Omega\Delta t \sim 0.3$ as expected from Ref. [1]), while the limit is $\omega_0\Delta t \sim 0.3$ for the Cyclotronic scheme: that is to say using the Cyclotronic scheme reduces the cost by a factor of Ω/ω_0 ($= 5\pi/3 \simeq 5$ in this case).

The vertical dashed line in Fig. 6 shows the Nyquist limit for the Modified Cyclotron frequency ($\omega_{\text{MC}}\Delta t = \pi$, where $\omega_{MC} \sim \Omega$).

5.2. Conservation properties

Fig. 7(a) shows the particle's energy ($W = W_K + W_P$, Kinetic + Potential energy) evolution for $\omega_0\Delta t = 0.2$. Neither of the two algorithms show a secular energy drift. Although the Boris scheme conserves energy better here than the Cyclotronic integrator, it is not a general rule and we have studied other test problems such as the magnetized Rydberg atom were the opposite holds. Because the fourth order Runge–Kutta scheme is not time-reversible, it does not conserve energy.

Fig. 7(b) shows the canonical angular momentum conservation (Eq. (13)) for the same parameters as in Fig. 7(a). When using the Cyclotronic integrator p_φ is exactly conserved. Indeed the Drift (Eq. (17)) is the mapping of a Larmor rotation and by

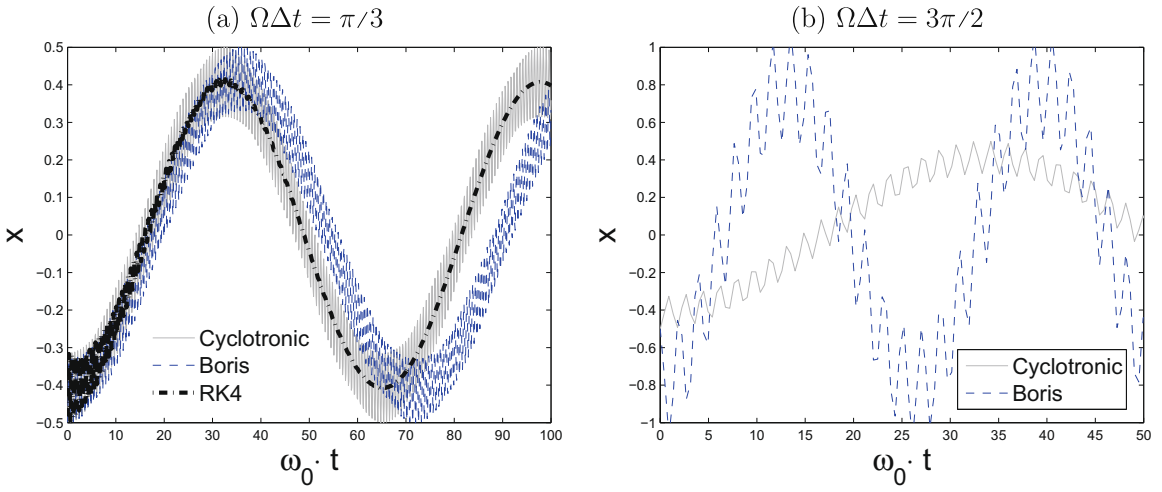

c) Angular frequencies corresponding to the curves in (a) and (b)

	Analytic	a (RK4)	a (Boris)	a (Cyclotronic)	b (Boris)	b (Cyclotronic)
ω_{MC}/ω_0	10.38	XX	10.39	10.38	XX	XX
ω_{Mag}/ω_0	$9.638 \cdot 10^{-2}$	$9.644 \cdot 10^{-2}$	$8.729 \cdot 10^{-2}$	$9.634 \cdot 10^{-2}$	0.2151	$9.782 \cdot 10^{-2}$

Fig. 5. **x**-position of the particle for the Boris push, the Cyclotronic integrator and the fourth order Runge–Kutta scheme, for the ideal Penning trap system. $\omega_0\Delta t = 1/10$ and $\Omega\Delta t = \pi/3$ (a). $\omega_0\Delta t = 9/20$ and $\Omega\Delta t = 3\pi/2$ (b). The ratio Ω/ω_0, only physically meaningful quantity, is equal in both cases. The initial conditions are $\mathbf{x} = (-0.5, 0, 0)$ and $\mathbf{v}/\omega_0 = (0, 1, 0)$. The fourth order Runge–Kutta scheme does not resolve the Cyclotron motion for the parameters of figure (a), and is unstable for the parameters of figure (b). The characteristic angular frequencies of the curves in (a) and (b) are printed in Table (c).

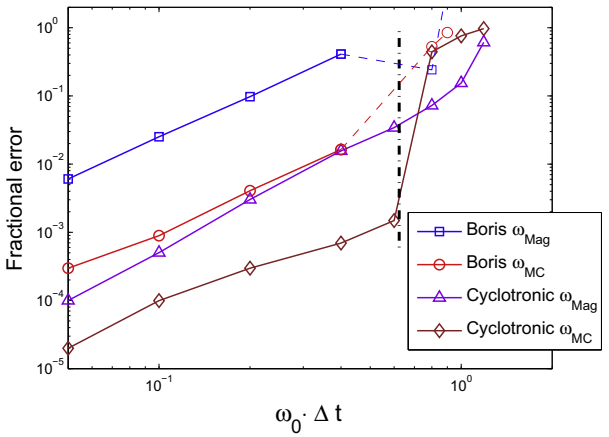

Fig. 6. Fractional error in the characteristic frequencies as a function of the time-step for the ideal penning trap system. ω_{Mag} is the magnetron angular frequency, and ω_{MC} the modified Cyclotron angular frequency. $\Omega/\omega_0 = 5\pi/3$.

definition conserves p_φ, and because of the cylindrical geometry of the potential the Kick (Eq. (18)) does not change v_φ. As expected the Boris integrator introduces an error in p_φ but no secular drift as opposed to the fourth order Runge–Kutta scheme.

5.3. Comparison of the Taylor expansion algorithm and the Cyclotronic integrator

Although unconditionally unstable, it is interesting to compare the Taylor expansion algorithm described in Section 4.4 with the Cyclotronic integrator for $\Omega\Delta t = O(1)$.

Fig. 8(a) shows the particle position projected on the **x**-direction with parameters $\Omega\Delta t = \pi$ and $\omega_0\Delta t = 0.2$, with initial conditions $\mathbf{x} = (-0.5, 0, 0)$ and $\mathbf{v}/\omega_0 = (0, 1, 0)$. While the trajectory computed using the Cyclotronic integrator is bounded,

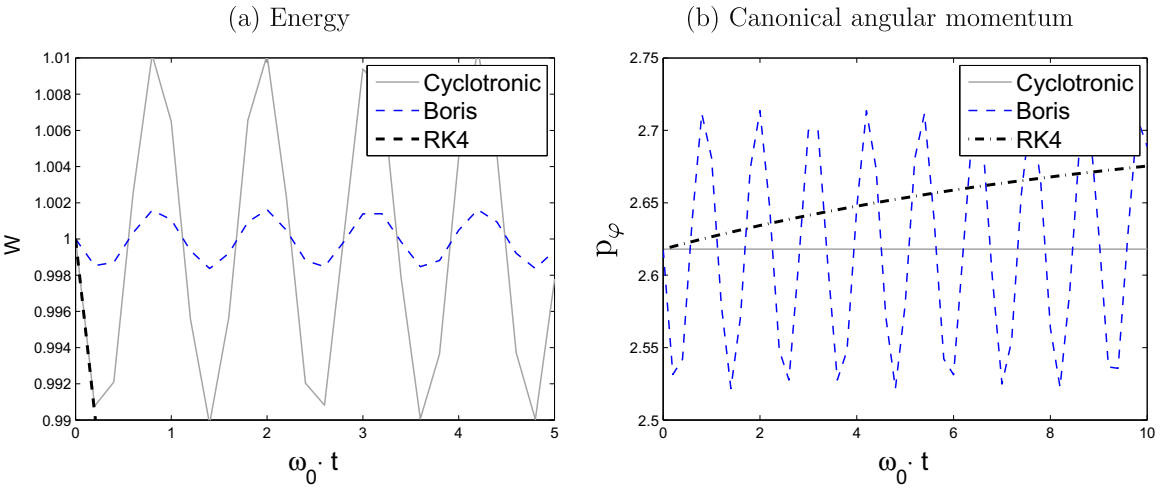

Fig. 7. Time evolution of the energy (a) and canonical angular momentum (b) for the ideal penning trap system, with $\Omega\Delta t = \pi/3$ and $\omega_0\Delta t = 0.2$. The initial conditions are $\mathbf{x} = (1,0,0)$ and $\mathbf{v}/\omega_0 = (1,0,0)$.

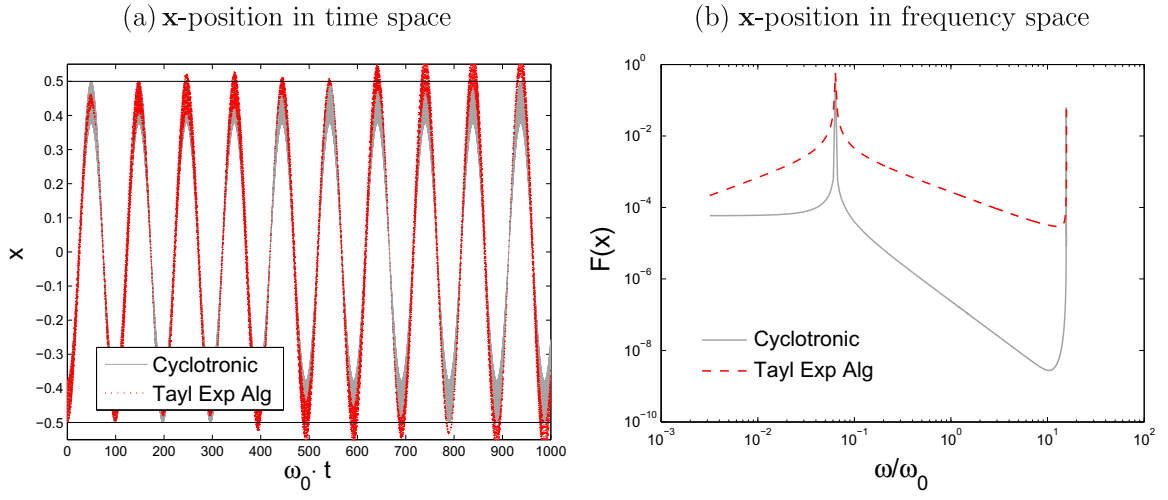

Fig. 8. (a) shows the **x**-position evolution with time for the ideal penning trap system, with $\Omega\Delta t = \pi$ and $\omega_0\Delta t = 0.2$. The initial conditions are $\mathbf{x} = (-0.5,0,0)$ and $\mathbf{v}/\omega_0 = (0,1,0)$. (b) is the Fourier transform of (a) carried on 20 Magnetron periods. The high-frequency peak has little meaning since the sampling frequency is exactly equal to the Nyquist frequency for the Larmor motion. The low-frequency peak (Magnetron frequency) is identical for both the Cyclotronic integrator and the Taylor expansion algorithm. The unstability of the Taylor expansion algorithm appears in (b) as the non negligible Fourier weight of non resonant frequencies.

such is not the case when using the Taylor expansion algorithm. As shown in Fig. 8(b) both schemes compute the same characteristic frequencies; the spectrum associated with the Taylor expansion algorithm is however "polluted" by its instability.

6. Application 2: implementation in SCEPTIC

In PIC codes, the electric field is calculated self consistently with the position of a large number of particles; it is therefore essential to resolve the plasma angular frequency $\omega_p = \sqrt{nQ^2/m\epsilon_0}$ (Q and m are the particles' charge and mass, and n is their density). Plasma oscillations are very similar in nature to the motion in a Penning trap, since the plasma frequency can be rewritten as $\omega_p = \sqrt{|Q\nabla^2\phi|/m}$ with $\nabla^2\ \phi = Qn/\epsilon_0$, while dimensionally the Penning trap harmonic frequency is $\omega_0 \sim \sqrt{|Q\partial^2\phi/\partial r^2|/m}$ with ϕ given by Eq. (19). The ideal Penning trap is therefore a key test problem in assessing the suitability of an integrator to PIC codes, where stability and energy conservation are perhaps even more important than in an orbit integration exercise.

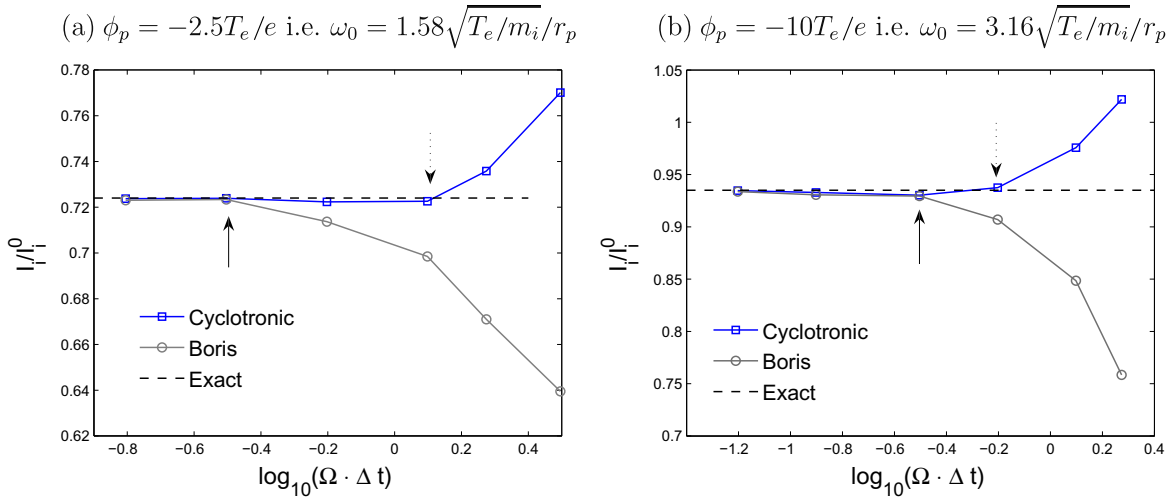

Fig. 9. Ion current I_i to the probe against $\Omega\Delta t$, normalized by the random thermal current $I_i^0 = 4\pi r_p^2 v_{ti}/(2\sqrt{\pi})$ ($v_{ti} = \sqrt{2T_i/m_i}$ being the ion thermal speed). The simulations parameters are $T_i = T_e$, $\Omega = 6.3\sqrt{T_e/m_i}/r_p$, $\lambda_{De} = 3r_p$ and $v_d = 0.5\sqrt{T_e/m_i}$. The dashed and solid arrows indicate the time-step at which 1% accuracy on the ion current is reached with the Cyclotronic or Boris integrator. Two probe potentials are considered, leading to $\Omega/\omega_0 \simeq 4$ (a) and $\Omega/\omega_0 \simeq 2$ (b).

Those are however not the only desired properties of an integrator; when studying the current collection by an electrode for instance, also of importance is how accurately the particles' trajectories are integrated close to the collector. As a second benchmark of the Cyclotronic integrator, we now discuss its implementation in the kinetic code SCEPTIC, designed to study plasma flows past a spherical probe. A detailed description of the code in the collisionless magnetized regime can be found in Refs [6,7]. One of its key features is a Boltzmann description of the electrons, hence only the ions (charge e and mass m_i) are advanced according to Eq. (1).

We take as larger characteristic angular frequency $\omega_0 = \sqrt{|e\partial E/\partial r|_p/m_i}$, where $|\partial E/\partial r|_p$ is the radial electric field derivative at the probe surface. For sufficiently large Debye lengths, $|\partial E/\partial r|_p = |\phi_p|/r_p^2$ [7], where ϕ_p and r_p are the probe bias and radius.

Fig. 9 shows the evolution of the ion current I_i to the probe computed by SCEPTIC as a function of the time-step Δt, with either Boris or the Cyclotronic integrator. The parameters used are $T_i = T_e$ (equal ion and electron temperatures), $\lambda_{De} = 3r_p$ (electron Debye length) and $\Omega = 6.3\sqrt{T_e/m_i}/r_p$. Furthermore, we assume that at infinity (i.e. far from the probe) the plasma is flowing with a drift velocity $v_d = 0.5\sqrt{T_e/m_i}$ parallel to the magnetic field.

It can be seen from Fig. 9 that regardless of the probe bias, when using Boris integrator, $\Omega\Delta t \lesssim 0.3$ is required for a 1% accuracy as predicted in Section 5.1. Achieving the same accuracy using the Cyclotronic integrator only requires $\omega_0\Delta t \lesssim 0.3$, in conformity with our expectations as well.

For the parameters of Fig. 9(a) using the Cyclotronic integrator reduces the cost by $\Omega/\omega_0 \simeq 4$, while the cost reduction in Fig. 9(b) is $\Omega/\omega_0 \simeq 2$. For higher magnetic fields or smaller probe bias, the benefit is limited to a factor of ten; indeed the stability limit is $\Omega\Delta t < \pi$, approximately ten times larger than the Larmor constraint for the Boris scheme $\Omega\Delta t \lesssim 0.3$.

It is important to mention that in this illustration the magnetization is rather high (average ion Larmor radius at infinity $r_L = \sqrt{\pi T_i/2m_i}/\Omega = 0.2r_p$), and additional effects such as ion-ion Coulomb collisions are likely to affect the collisionless results shown in Fig. 9.

The Cyclotronic integrator has also successfully been implemented in a recent version of the full PIC code Democritus [8].

7. Summary and conclusions

The orbit integrator is a key ingredient in Particle In Cell codes and special care must be used in its choice, in particular because particle advance is usually the most expensive step. The present publication is devoted to explicit schemes in the presence of a background homogeneous magnetic field.

Because it is time-reversible, the Boris integrator (Eqs. (2) and (3)) is well known for its long term conservation properties. It however suffers from the need to accurately resolve the Larmor frequency, which is inefficient if it is much larger than any other characteristic frequency of the problem.

In order to dodge the Larmor constraint, Spreiter and Walter developed a particle mover in which the constant uniform magnetic field is built in the propagation equations (Section 4.4). This algorithm is very attractive if the problem allows time-steps much longer than the Larmor period [16], but too unstable otherwise (Fig. 4). In addition, it does not exactly conserve energy, which could be a problem if used in codes where long-term particle tracking is necessary.

The central message of this publication is that we have developed a new orbit integrator not subject to the Larmor constraint, which is second order accurate and symplectic (hence time-reversible) when the magnetic field is static and uniform; provided the non-magnetic characteristic frequencies are accurately enough resolved, only the linear stability condition $\Omega\Delta t < \pi$ must be satisfied (Fig. 3). The Cyclotronic integrator can easily be implemented in leap-frog style as illustrated by Eqs. (17) and (18), thus requiring only one field-evaluation per time-step.

The Cyclotronic integrator has successfully been implemented in the electrostatic PIC codes SCEPTIC [6,7] and in recent versions of Democritus [8], where the cost of orbit integration has been reduced by up to a factor of ten.

Acknowledgments

Leonardo Patacchini was supported in part by NSF/DOE Grant No. DE-FG02-06ER54891. The SCEPTIC calculations are performed on the Alcator Beowulf cluster which is supported by US DOE Grant No. DE-FC02-99ER54512. The implementation of the Cyclotronic integrator in Democritus was performed in collaboration with Giovanni Lapenta.

References

[1] C. Birdsall, A. Langdon, Plasma Physics via Computer Simulation, McGraw-Hill, New York, 1985.
[2] V. Fuchs, J.P. Gunn, On the integration of equations of motion for particle-in-cell codes, J. Comput. Phys. 214 (2006) 299–315.
[3] R.I. McLachlan, M. Perlmutter, Energy drift in reversible time integration, letter to the editor, J. Phys. A 37 (2004) 45.
[4] Q. Spreiter, M. Walter, Classical molecular dynamics simulation with the Velocity Verlet algorithm at strong external magnetic fields, J. Comput. Phys. 152 (1999) 102–119.
[5] D. Donnelly, E. Rogers, Symplectic integrators: an introduction, Am. J. Phys. 73 (2005) 10.
[6] L. Patacchini, I.H. Hutchinson, Angular distribution of current to a sphere in a flowing, weakly magnetized plasma with negligible Debye length, Plasma Phys. Control. Fusion 49 (2007) 1193–1208.
[7] L. Patacchini, I.H. Hutchinson, Ion-collecting sphere in a stationary, weakly magnetized plasma with finite shielding length, Plasma Phys. Control. Fusion 49 (2007) 1719–1733.
[8] G. Lapenta, Simulation of charging and shielding of dust particles in drifting plasmas, Phys. Plasmas 6 (1999) 1442–1447.
[9] D.H.E. Dubin, T.M. O'Neil, Computer simulation of ion clouds in a Penning trap, Phys. Rev. Lett. 60 (1988) 6.
[10] H. Kinoshita, H. Yoshida, H. Nakai, Symplectic integrators and their application to dynamical astronomy, Celestial Mech. Dyn. Astr. 50 (1991) 59–71.
[11] E. Forest, Geometric integration for particle accelerators, J. Phys. A 39 (2006) 5321–5377.
[12] P.G. Hjorth, N. Nordkvist, Classical mechanics and symplectic integration, Unpublished notes available on line: <http://www2.mat.dtu.dk/people/N.Nordkvist/lecture_notes.pdf>.
[13] P.H. Stoltz et al, Efficiency of a Boris-like integration scheme with spatial stepping, Phys. Rev. Special Topics – Accelerators Beams 5 (2002) 094001.
[14] W.W. Lee, W.X. Wang, W.M. Tang, et al, Gyrokinetic particle simulation of fusion plasmas: path to petascale computing, J. Phys.: Conf. Series 46 (2006) 73–81.
[15] L.S. Brown, G. Gabrielse, Geonium theory: physics of a single electron or ion in a Penning trap, Rev. Modern Phys. 58 (1986) 233–311.
[16] F. Herfurth, S. Eliseev, et al, The HITRAP project at GSI: trapping and cooling of highly-charged ions in a penning trap, Hyperfine Interact. 173 (2006) 1–3.